

Exercise-induced effects on a gym atmosphere

Abstract We report results of analysis of a month-long measurement of indoor air and environment quality parameters in one gym during sporting activities such as football, basketball, volleyball, badminton, boxing, and fitness. We have determined an average single person's contribution to the increase of temperature, humidity, and dust concentration in the gym air volume of 12500 m³: during 90-min exercise performed at an average heart rate of 143 ± 10 bpm, a single person evaporated 0.94 kg of water into the air by sweating, contributed 0.03 K to the air temperature rise and added 1.5 µg/m³ and 5 ng/m³ to the indoor concentration of inhalable particles (PM₁₀) and Ca concentration, respectively. As the breathing at the observed exercise intensity was about three times faster with respect to the resting condition and as the exercise-induced PM₁₀ concentration was about two times larger than outdoors, a sportsman in the gym would receive about a sixfold higher dose of PM₁₀ inside than he/she would have received at rest outside.

**M. Žitnik^{1,2}, K. Bučar¹, B. Hiti¹,
Ž. Barba¹, Z. Rupnik¹, A. Založnik¹,
E. Žitnik³, L. Rodriguez⁴,
I. Mihevc⁵, J. Žibert⁶**

¹Jožef Stefan Institute, Ljubljana, Slovenia, ²Faculty of Mathematics and Physics, University of Ljubljana, Ljubljana, Slovenia, ³Faculty of Medicine, University of Ljubljana, Ljubljana, Slovenia, ⁴Centro Atómico Bariloche, CNEA and CONICET, Bariloche, Argentina, ⁵Faculty of Electrical Engineering, University of Ljubljana, Ljubljana, Slovenia, ⁶Institute Andrej Marušič, University of Primorska, Koper, Slovenia

Key words: Indoor air quality; Physical exercises; Perspiration; Particulate matter; Temporal resolution; PM₁₀.

M. Žitnik
Jožef Stefan Institute, P.O. Box 3000, SI-1001, Ljubljana
Slovenia
Tel.: +386-1-5885374
Fax: +386-1-5885255
e-mail: matjaz.zitnik@ijs.si

Received for review 25 November 2014. Accepted for publication 6 June 2015.

Practical Implications

Sporting activities occupy considerable time in the schedule of humans engaged in long periods of sedentary work in industrialized countries. While health impacts of exercises per se are indisputably beneficial, activity in polluted air may not be productive. In this respect, it is important to investigate busy indoor gyms where a mixture of exercise-induced humidity, temperature, and particulate matter concentration may result in higher than average levels which become a heavy burden for human respiratory systems operating at a higher rate.

Introduction

A wealth of epidemiological data supports the hypothesis that on average, for every 10 µg/m³ rise of total mass concentration of inhalable particles (PM₁₀) in the air, there is an increase of about 1% in cardiovascular mortality on a day-to-day basis (Routledge and Ayers, 2006). This assessment is primarily made on the basis of measured outdoor PM₁₀ concentration, although humans in industrialized countries spend 80–90% of their time indoors (Klepeis et al., 2001; Schweizer et al., 2007). The quality of the indoor air and environmental quality (IEQ) in terms

of gas-phase constituents and particulate matter composition may differ substantially from the corresponding outdoor values (Mitchell et al., 2007; Seppänen et al., 1999), and the significance of this fact has triggered many field studies (See and Balasubramanian, 2008; Gehin et al., 2008; Martuzevicius et al., 2008; Sotiriou et al., 2008; Kuo et al., 2007; Žitnik et al., 2010; Bennett et al., 2012; Salma et al., 2013).

It is especially interesting to study the concentration levels of particulate matter (PM) in the gym, where a significant contribution of inhalable fraction (PM₁₀) is expected to be self-induced by physical exercises, caus-

ing at the same time an increase in exposure to inhaled aerosols due to increase of pulmonary ventilation during exercises. Initial studies along these lines were performed in three elementary school gyms (Branuš et al., 2009, 2011). The observed increase of the coarse PM fraction (PM_{10} – $PM_{2.5}$) relative to the outdoor level was attributed to the human activity because the signal was well correlated with the number of exercising people and hours spent in the gym. The analysis of the indoor aerosol samples taken with 24-h collection time shows that besides crustal material, mite debris and mold fibers, and skin scales were the most frequent contributors to dust particles. Buonanno et al. (2012) observed 4.8 ± 2.0 times higher average coarse particle concentrations with respect to the background (outdoor) values in 12 school gyms using natural ventilation. The total energy expended by the pupils was identified as a key parameter to describe dust resuspension effect, characterized by the observed median emission factor of $67 \mu\text{g}/\text{min}/\text{pupil}$. A correlation of the measured CO_2 concentration with the amount and intensity of physical activity was also pointed out: a 100 ppm increase of CO_2 concentration in the gym was reported to correspond to about $13 \mu\text{g}/\text{m}^3$ rise of concentration of the coarse PM fraction. A recently published study of exposure to indoor air pollutants during physical activity in fitness centers showed that highest detected PM_{10} concentrations (100 – $200 \mu\text{g}/\text{m}^3$) were coincident with the period of fitness classes and that measured CO_2 concentration levels also depended on the type of activity (Ramos et al., 2014). The studies of Sacks and Shendell (2014a,b) also report excessive values of PM_{10} and CO_2 concentration during physical activities in a local gym. Their results indicate that in order to reduce exposure to air pollutants and reach the thermal comfort range it is crucial to optimize air conditioning systems in terms of ventilation rate, air drying, and air filtering.

As the gym's IEQ parameters depend on cleanliness, type and intensity of physical activity, quality of the ventilation system, and on sources of pollution outside the schools, it is difficult to generalize the results and more studies of this kind are needed, especially those with high temporal resolution. Any gym, in fact, is characterized by the unfortunate situation where physical activity triggers both dust generation and an increase of the pulmonary ventilation creating potentially hazardous situations in terms of an extra PM_{10} exposure, which in turn may reduce benefits of physical activity on human health. In addition, due to exercise, water vapor is released into the air which may affect relative humidity and aerosol formation (Fromme et al., 2007).

To obtain more answers to these important questions, we describe here the study of exercise-induced IEQ of a gym such as air temperature, relative humidity, and PM_{10} concentration, which were sampled with

one-minute time resolution, much shorter than the typical exercise time slot of 90 min. Special care is taken to compare the indoor data with the simultaneously measured outdoor data to allow for a reliable identification and quantification of the contribution of human activity to the increase of indoor air humidity and PM_{10} concentration. In addition, concentration trends of several elements (Ca, Fe, Si) in the PM were determined by analyzing hourly dust samples by proton-induced X-ray emission (PIXE). We have also followed the type of physical activity and assessed overall effects of physical exercises on the gym air temperature.

Methods

Sampling sites

The sampling period lasted from March 2 to April 4, 2011 and for the study of indoor atmospheric parameters, the gym hall in Rožna Dolina, Ljubljana, Slovenia (N46°03'04.10", E014°29'13.53") was chosen (Figure 1a). At this place, a regular working day-to-day recreational activity for students of the University of Ljubljana is organized and supervised by professional employees. Sports games such as basketball, volleyball, football, badminton, and boxing were performed on three parallel exercise areas (A, B, and C), each of $14.7 \times 25.1 \text{ m}^2$ surface (Figure 1b). A typical exercise time slot lasted 90 min and started with warm-up activities. As seen in Figure 1b, the

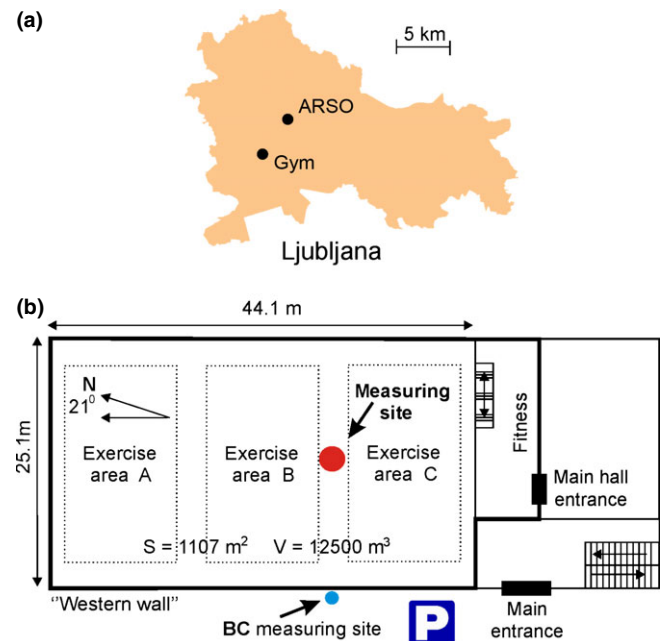


Fig. 1 (a) Location of the gym and of the official ARSO measuring site in the Ljubljana urban area. (b) Scheme of the gym interior giving orientation of the building and its dimensions, as well as position of the indoor (large red circle) and of the outdoor (small blue circle) measuring site

measuring site was situated between areas B and C and the signals were acquired at 2 m height from the gym floor.

The gym IEQ was affected by heat, humidity, and dust exchange with the atmosphere outdoors, the transport being mediated by the gym walls and by the gym heating/ventilation system (HVAC). To isolate sporting activity markers, simultaneous acquisition of outdoor reference values of temperature, relative humidity, and PM₁₀ concentration was of utmost importance. The relevant data, together with solar radiation data, were measured at the nearby official measuring site of the Environmental Agency of Slovenia (N46°03'55.76", E014°30'44.71").

Instrumentation

The indoor measuring site consisted of a metal construction protected by a plastic net which hosted an AMES meteorological station with internal memory for storage of the acquired air temperature and relative humidity data, a commercial instrument Teom 1400A for PM₁₀ sampling (Hansen et al., 1984) and a 2D-step sampler. The latter was developed at Tohoku University (Matsuyama et al., 2003) to collect a sequence of hourly dust samples on a Nuclepore filter sheet suitable for elemental concentration analysis. Altogether 735 dust samples were collected by the 2D-step sampler. In short, when an air pump is switched off, a small reversible motor moves the suction nozzle, placed just below the filter surface, to a new sample position on a filter, 5 mm from the center of the previous spot. The 160 × 160 mm² filter surface is large enough to hold about a thousand aerosol samples. A clean filter sheet was cut out of the Nuclepore circular substrate with 293 mm diameter and 1 μm pore sizes. When in position, the pump is switched on for a preset sampling time (1 h in our case) to extract 1 l/min of air through the nozzle with 2 mm diameter. A needle valve kept the air mass flow stable and a programmable controller switched between the nozzle movement and pump operation.

At the outside measuring site (Figure 1b), a 2-channel (UV+IR) Aethalometer (Magee Scientific, AE 42-2-ER-P3) was simultaneously measuring black carbon (BC) concentration with one-minute time resolution to identify possible local outdoor BC sources.

Exercise intensity

Besides the number of persons attending each exercise, it is important to determine exercise intensity in order to place the relation between physical activity and the gym's IEQ parameters on a more quantitative basis. For this purpose, we have measured average heart rate of randomly selected students during their exercises using standard heart rate monitors Polar RS 800,

S610, RS300, FT7, and F7. Altogether 193 students volunteered to submit to the test in the March 15–31, 2011 period: 153 male and 40 female, with a group average age of 22.3 ± 1.9 years. Each exercise started with a 20–30-min warm-up period followed by a 45-min period of games of either basketball (3:3, 4:4 and 5:5), football (futsal) (4:4), and volleyball (6:6), or fitness, and the average heart rate F_s of individuals was read out at the end of the exercise. The average heart rate was found to be $\langle F_s \rangle = 143 \pm 10$ bpm, and the average exercise effort, defined by an average of $F_s/(220 - \text{age}[\text{years}])$, was $71 \pm 5\%$.

Sampling analysis

Air humidity. The relative humidity H does not directly determine the water vapor density in the air. The latter is given by $\rho(T) = p(T)/(MRT)$ where $p(T) = HP(T)$ is the water vapor pressure. The saturated vapor pressure P at temperature T was estimated by the Clausius–Clapeyron equation:

$$P(T) = P_0 e^{-T_0/(\frac{1}{T} - \frac{1}{T_r})}, \quad (1)$$

where $T_r = 373.15$ K, $P_0 = 101.3$ kPa, and $T_0 = 5100$ K $\approx Mq_r/R$ were set so as to obtain good agreement with Koutsoyannis (2012). For 1 kmol of air $M = 29$ kg, the heat of vaporization of water at temperature T_r is $q_r = 2.260$ MJ/kg and the gas constant is $R = 8314.46$ J/kmol/K.

The outdoor–indoor vapor pressure difference $p_o - p_{io}$ causes water transfer. The indoor atmosphere acts as an externally driven reservoir, so that the outdoor vapor pressure p_o fully determines the behavior of p_{io} with time. Similar to thermal transport, water transport is assumed to obey a linear law according to which the change of the vapor pressure per unit of time is proportional to the pressure difference, $dp_{io}/dt = \tau_p^{-1}(p_o - p_{io})$. The corresponding relaxation time $\tau_p \approx 20$ h was found by fitting the simulated curve $p_{io}(t)$ to the measured data during the weekends with no human activity in the gym. In this model, p_{io} is in fact a smoothed version of the external water vapor pressure trend p_o with a small time delay due to the finite velocity of the water transport through the gym walls. This simple model deals with an inert wall, that is, the water flux on both sides of the wall is equal at all times, and it assumes that the air inside is well mixed on a timescale much shorter than τ_p . Once τ_p is selected, one can generate a hypothetical trend of water vapor pressure p_{io} inside the gym assuming no internal sources of water. As seen in Figure 3, most of the time p_{io} is smaller than $p_i = H_i P(T_i)$, the ‘measured’ indoor vapor pressure that is constructed from the measured relative humidity H_i and temperature T_i inside the gym, except at a few points

where the simulated profile is forced to match the measured profile to avoid instability of the model.

In the next step, we analyzed $p_h = p_i - p_{io}$, the extracted trend of the human contribution to the water vapor in the gym. Our goal was to determine the underlying water source strength as a function of time in order to explain the observed variability of p_h . This is modeled by the following differential equation: $d\bar{p}_h/dt = -\tau_n^{-1}\bar{p}_h + N(t)C$, where N is the number of people in the gym and C denotes the mass of water generated per person per unit of time. The solution for $t \geq 0$ is

$$\bar{p}_h = N(t)C + (\bar{p}_h(0) - N(t)C)e^{-t/\tau_n} \quad (2)$$

where $\bar{p}_h(0)$ is an initial vapor pressure value. The analysis of the p_h trend shows that $\tau_n = 6$ h is suitable to describe the water vapor pressure drop during the night following an active day period. This is much faster than the ‘weekend’ time constant τ_p because the water sources to which the indoor atmosphere reacts are inside the gym while the external changes of humidity are damped by the gym wall acting as a low pass filter. Moreover, during an active period of the day one notes that even sharper vapor pressure drops were recorded ($\tau_2 \approx 1.4$ h) and this is attributed to the local water vapor generation and air mixing action of the exercising people. Taking these considerations into account, the form of Equation 2 is employed to perform a piecewise fit of the p_h trend with the following functional dependence:

$$\bar{p}_h(t) = \sum_i (N_i C_i + (\bar{p}_{h,i}(t) - N_i C_i) e^{-t/\tau_s}), \quad (3)$$

where $\tau_s^{-1} = \tau_n^{-1} - \tau_2^{-1}(1 - \delta_{0,N_i})$ and $\bar{p}_{h,i}$ are nonzero only in the time interval $t_i \leq t \leq t_{i+1}$ and $\bar{p}_{h,i}(t_i) = \bar{p}_{h,i-1}(t_i)$. We have also tried to perform the fit by further decomposing the source according to the activity fingerprint (Figure 2), that is, by subdividing the total number of exercising people in a given $\Delta t = 90$ -min exercise time interval according to different exercise types $N_i = \sum_a N_{i,a}$ and assigning to each type its own ‘sweat’ constant C_a , effectively replacing $N_i C_i$ by $\sum_a N_{i,a} C_a$ in Equation 3. It turned out that such attempts did not lead to stable results.

Air temperature. The air temperature in the gym was expected to reflect exercising activities too, although it turned out that the relation between the two is more difficult to isolate than in the case of humidity because of a larger variety of heat sources, such as internal heating and external site-specific solar radiation. To estimate an average single person’s contribution to the increase of the indoor temperature, an approach similar to the one in the previous subsection was employed. The parameters governing heat transfer

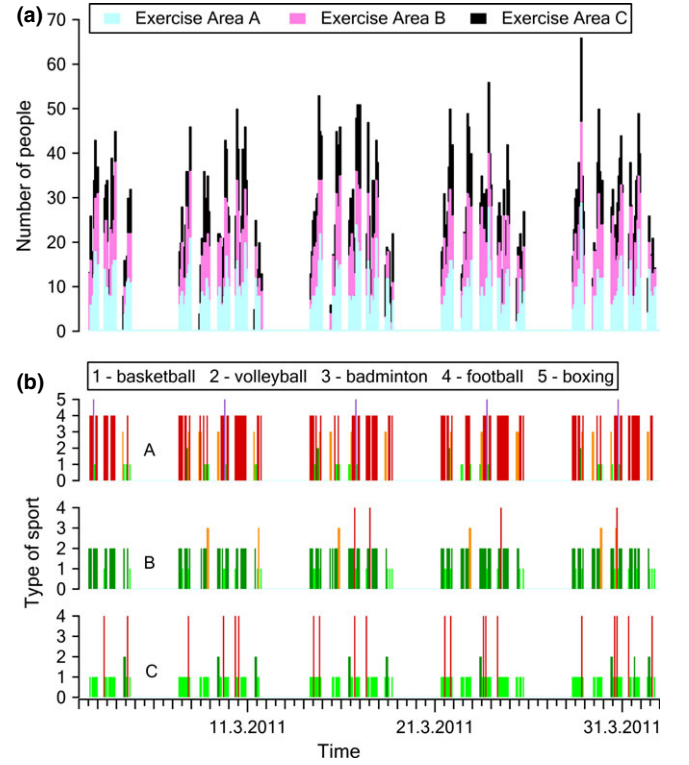


Fig. 2 (a) The number of people practicing in the exercise areas A, B, and C. (b) Type of sport practiced on areas A, B, and C as a function of time

were determined by analyzing the measured outdoor and indoor temperature trends during the weekends with no human activity in the gym and with the heating switched off. Essentially, the base model relies on a time-discretized heat transfer equation with a temporal resolution δt of one minute. For an empty gym with the central heating switched off, the indoor temperature $T_{oi}(n+1)$ at a time $(n+1)\delta t$ is calculated from temperatures $T(n)$ determined at a previous time $n\delta t$ by

$$T_{oi}(n+1) = T_{oi}(n) + \alpha(T_o(n) - T_{oi}(n)) + \gamma(T_R(n) - T_{oi}(n)), \quad (4)$$

where α represents a heat leakage through the gym walls (thermal conductance), T_o is the measured outside temperature, T_R is the temperature of a fictitious heat reservoir (heat stored in the walls, etc. with a slower cooling and/or heating rate than air), and γ represents coupling of the heat reservoir to the indoor air. The three model parameters α , γ and T_R were determined by fitting the generated temperature trend T_{oi} to the indoor temperature trend measured during the weekends. The same form (4) with fixed values of α , γ and T_R and an extra $\beta ctr(n)$ term on the left to describe the effect of central heating was employed to generate the expected indoor temperature trend without exercising people throughout the rest of the week. Parameters

β and $ctr(n)$ are the furnace power and the on/off control, respectively. The latter is equal either to 0 or 1, and its temporal evolution was determined manually by searching for the sharpest temperature rises of the measured indoor signal, excluding the evening time intervals where the temperature spikes are attributed to direct solar irradiation (see below). It is known that on working days the heating switched on every morning at 7:00 AM before the start of the first exercise time slot at 7:30 AM and was switched off after reaching the high temperature threshold value on a given sensor. During the day, the heating went on occasionally when the sensor temperature dropped below the low threshold value.

PIXE analysis of PM₁₀ samples. The irradiation of aerosol samples was performed at the external ion beam-line attached to the Tandatron accelerator facility at the Microanalytical Center (MIC) of the Jožef Stefan Institute in Ljubljana, Slovenia. The 2.5 MeV proton beam with 1 mm diameter passed through a metallic grid with 50% transmission before exiting the vacuum through an 8 μm thick Al foil to hit the sample spot placed 52 mm away from the beamline exit. X-ray emission from the sample spot was measured by a SiLi detector placed at an angle of 45° backwards with respect to the incoming proton beam and 52 mm away from the target. Using 5 nA proton current, a single spot X-ray spectrum was acquired in 7 min. The relative proton dose delivered to different sample spots was extracted from the yield of Ar K-L₂₃ emission lines. This signal originates from a quasi stable Ar concentration in the air, and its time integral is well proportional to the acquired proton dose. An absolute calibration of the x-ray spectra over a wide energy region was enabled by recording the spectra of several standard thin layer target materials (Rh, Y, Ge, Cu, Fe, Ti, CaF₂, KCl, CuS_x, SiO) with known $\sim 50 \mu\text{g}/\text{cm}^2$ surface density deposited on a Nuclepore substrate (Micromatter standard). The standard foils were attached to the same filter sheet and brought to the central position with respect to the beam. Computer-controlled movements automatically placed the table with the filter frame with the center of the next sample spot at the beam center when the spectrum acquisition of the previous spot was performed. Concentration levels due to possible filter sheet contamination were determined by collecting spectra at several unexposed filter areas. The corresponding 'background' average concentration levels were subtracted from data before further analysis. The elemental yields at different spots were extracted from the spectra by the GUPIX code (Campbell et al., 2010) and converted into the corresponding surface mass densities in the so-called thin target approximation which neglects proton beam energy loss and X-ray absorption in the target using known

atomic cross-sections, experimental geometry, and spectrometer characteristics.

Results and discussion

Exercise intensity

According to basic exercise physiology, at ~ 140 bpm heart rate, the pulmonary ventilation is expected to increase for about a factor of three with respect to resting conditions, due to both an increase of the respiratory rate and of the tidal volume. Knowing the heart rate, one can estimate the average power generated by a single person's metabolism. This is related to oxygen consumption: at rest, a typical oxygen consumption is ~ 0.27 l/min and basic metabolism produces about 95 W heat load per person (=1 MET, assuming that 1 liter of oxygen burning releases 21 kJ of energy). With the heart rate increasing to ~ 140 bpm, the volume flow of blood increases from 5 l/min to about 20 l/min, and the person works at about 60% of the maximal oxygen uptake $\text{VO}_{2\text{max}}$. This means that on average, for our group of students, the oxygen uptake was about $\text{VO}_2 \sim 2$ l/min, resulting in 150–200 W average mechanical power output to perform exercises, and 500–550 W of heat load that was dissipated to the environment to prevent body overheating. This estimate is fully consistent with 6–7 MET of the work metabolic rate generally expected for playing of soccer and basketball, according to the 2011 compendium of physical activities (Ainsworth et al., 2011).

It is known that for persons at rest a major part of heat is dissipated by radiation if the temperature of the environment is lower ($\sim 21^\circ\text{C}$) than the skin (clothes) temperature ($\sim 34^\circ\text{C}$). Other processes such as heat convection and perspiration would together amount to less than $\sim 20\%$ of the cooling. During exercises, the heat load increases and evaporative cooling due to sweating (perspiration) becomes the primary dissipative mechanism, as radiative cooling cannot increase substantially because the skin temperature is limited due to thermoregulatory mechanisms of the body. Assuming $\sim 37^\circ\text{C}$ skin temperature and 1.8 m² surface area of the human body acting like a perfect IR radiator, the radiative cooling can disperse up to 150 W of the heat load. The remaining 400 W must therefore be dissipated by water evaporation from the skin and by the convection. Although the convection is more efficient when the person is moving (air motion strips away the heated layer surrounding the skin), its cooling effect would still be smaller than the radiation cooling. During the exercises, a relatively small part of the heat output therefore goes into air heating; about 400 W per person is dissipated by evaporating water into the gym atmosphere.

Air humidity

A quick view of the measured data trends in Figure 3 indicates that the air humidity is the most obvious marker of people’s activity in the gym. By breathing, and mostly by sweating, a substantial amount of water vapor is generated during the exercises. This is reflected in measured levels of relative air humidity together with the residual ‘background’ water vapor. The two water vapor sources display very different dynamics, the former being evidently correlated with relatively fast hourly changes of the number of people practicing in the gym, and the latter changing smoothly on a daily timescale. To isolate the ‘human’ contribution to the overall humidity, the simultaneously measured outdoor humidity trend was employed to calculate the expected humidity levels inside the gym without people practicing. This simulated trend was subtracted from the measured humidity trend inside the gym to obtain the desired difference. Finally, the result was normalized to the actual people’s presence in the gym to determine an average water load of a single person exercising.

From our analysis, presented in Figure 4, we were able to extract a ‘sweat’ constant $\bar{C} = \langle C_i \rangle$, averaged over 400 exercise intervals that occurred during one month. Using the best C_i values, determined by the fit, $\bar{C} = 0.07$ Pa/min. This value is employed to calculate an average mass of water evaporated from a single

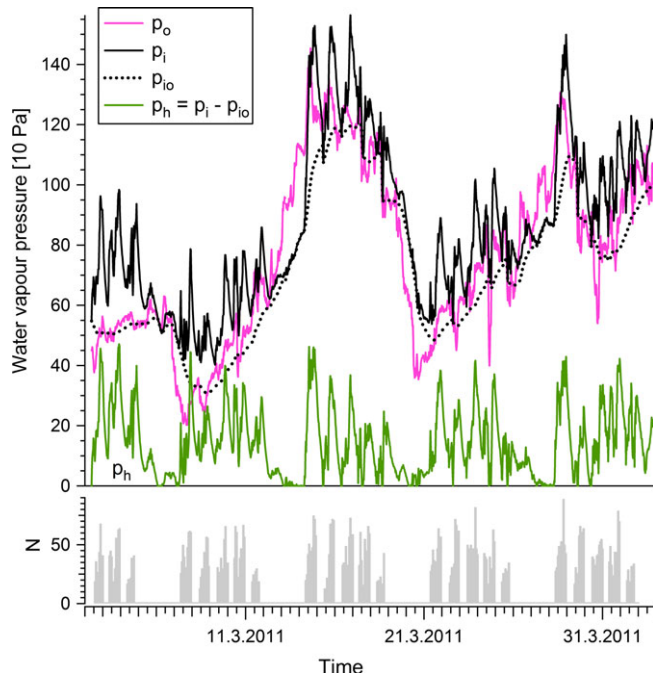


Fig. 3 Water vapor pressure as a function of time: outside the gym (p_o , gray (pink) solid curve), inside the gym (p_i , black solid curve), simulated inside the gym (p_{io} , dotted black curve), and the difference $p_i - p_{io}$ ((green), light gray solid curve). Histogram on the lower graph reports the number N of exercising people as a function of time

person per exercise time interval according to $m = M\bar{C}V\Delta t/(RT) \sim 0.94$ kg where $V \approx 12500$ m³ is the gym volume.

It is interesting to compare this result with the mass \bar{m} of water that needs to be evaporated to dissipate $\bar{P} \approx 400$ W of a single person’s heat load for a duration of an average physical exercise, as estimated above. We find that $\bar{m} = \bar{P}\Delta t/\bar{q} \approx 0.88$ kg, where $\bar{q} = 2.340$ MJ/kg is the latent heat of water vaporization at temperature of the skin. Although it is difficult to judge how homogeneous are the vertical profiles of air temperature and humidity in the gym from a single-point measurement, good agreement between the two results for the evaporated water mass lends credibility to both. Moreover, similar values of the sweat loss are reported in the literature (Shapiro et al., 1982), for example, 1.1 kg sweat loss in 90 min was detected when a subject was walking on a 5% treadmill grade with 1.34 m/s speed, wearing shorts, and at 35°C outside temperature and 75% relative humidity. The sweat loss at rest under the same environmental conditions was 0.44 kg and was subtracted to obtain the above value.

Air temperature

By subtracting the simulated indoor temperature from the measured indoor temperature, one is left with the temperature trend T_h that is still not entirely due to human activity (Figure 5). T_h shows sharp peaks occurring occasionally around 6 PM that could not be explained by the previously described mechanisms. We attribute their origin to the late afternoon sun shining almost perpendicularly to the 10 m high western wall of the gym which is to a large extent (~30%) covered by glass windows. To validate the hypothesis, we looked at the measured solar radiation trend for

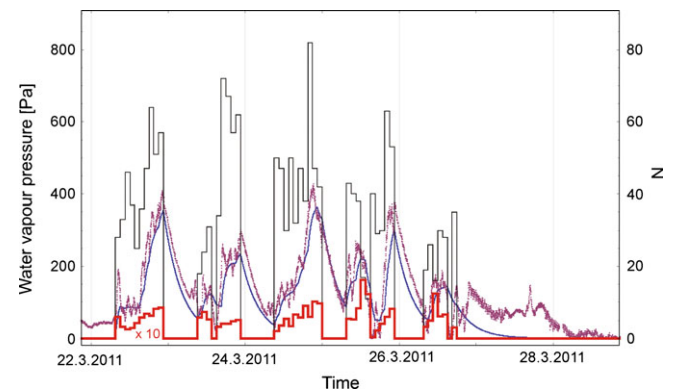


Fig. 4 Extracted human contribution p_h to the water vapor pressure for the March 22–28 period (violet, dots) compared to the piecewise fit result (blue, black solid curve). Reported are also a histogram of the number N_i of people exercising (black thin line) and a histogram of the single person’s contribution to the water vapor pressure $C_i\Delta t$ (red, gray thick line) in the exercise time slot Δt

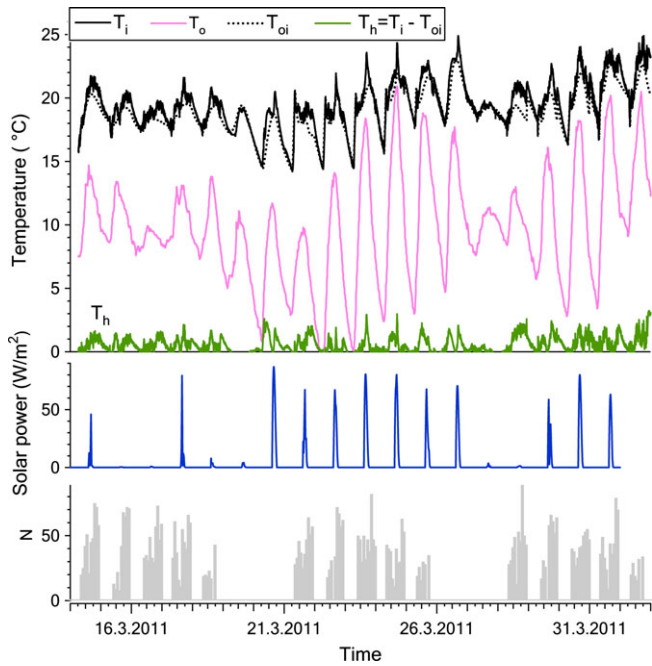


Fig. 5 Measured indoor temperature T_i (black) and outdoor temperature T_o (pink) together with the simulated trend T_{oi} corrected for the central heating (blue) and the difference between the measured indoor and simulated indoor temperature T_h (green). The latter corresponds to the effect of human exercise, except for the sharp evening peaks due to direct solar irradiation (blue) of the ‘western wall’ (Figure 1) of this study’s gym. Histogram on the lower graph reports the number N of exercising people as a function of time

Ljubljana and append to these data the calculated sun’s azimuth and altitude angles as a function of time. Consideration of the gym’s position and orientation in space revealed that only its western side can be strongly exposed to the direct sunlight as the other three sides are shaded by nearby objects and roof structures. Taking the data into account, one can calculate the actual solar flux incident on the western wall of the gym. Plotting the trend on the same timescale with the measured indoor temperature revealed a clear coincidence of previously unexplained temperature peaks with the maxima of the solar irradiation of the gym wall (Figure 5). It is found that the maximum power density absorbed by the gym western wall was of the order of 80 W/m^2 . It is easy to check that the corresponding heat power entering through the windows ($\sim 10 \text{ kW}$) is able to warm up the entire air in the gym by a couple of degrees in a matter of an hour, as indeed was observed (Figure 5). We assume that the major part of heat is dissipated by heating up the air which may be a reasonable approximation because large heated surfaces in the gym generate strong convection currents.

Averaging T_h over the exercise time slot and dividing by an average number of people exercising returns an average increase of the air temperature of $\Delta t = 0.03^\circ\text{C}$ per exercising person at the measuring point. If the air in the gym is well mixed, such a temperature change

would require $\rho V c_p \Delta T / \Delta t \approx 85 \text{ W}$ per person of direct air heating power, taking $\rho = 1.2 \text{ kg/m}^3$ for the density and $c_p = 1000 \text{ J/kg/K}$ for the specific heat of air. With an average number of people per exercise time slot $\bar{N} = 38$, the whole group represents a source of $\sim 6 \text{ kW}$ power radiating mainly in the infrared. Similar to the solar irradiation case, this would lead to an overall temperature rise of $\sim 1 \text{ K}$, as was indeed observed. Another possible mechanism for warming-up the gym atmosphere would be mixing of the ‘hot’ water vapor, characterized by a large specific heat 186 MJ/kg , with the ‘cold’ air at $\sim 21^\circ\text{C}$. However, a good agreement of the exercise warm-up effect with the solar irradiation warm-up effect suggests that the water vapor is released from skin practically at the same temperature as the surrounding air. The convection triggered by heated bodies and warmed-up gym walls is a major heat-up mechanism of air. A direct warm-up by absorption of IR radiation is less efficient because the attenuation length for 293 K black body radiation (centered in the $8\text{--}12 \mu\text{m}$ wavelength region) in the air is as large as 6.6 km (Rothman et al., 2009).

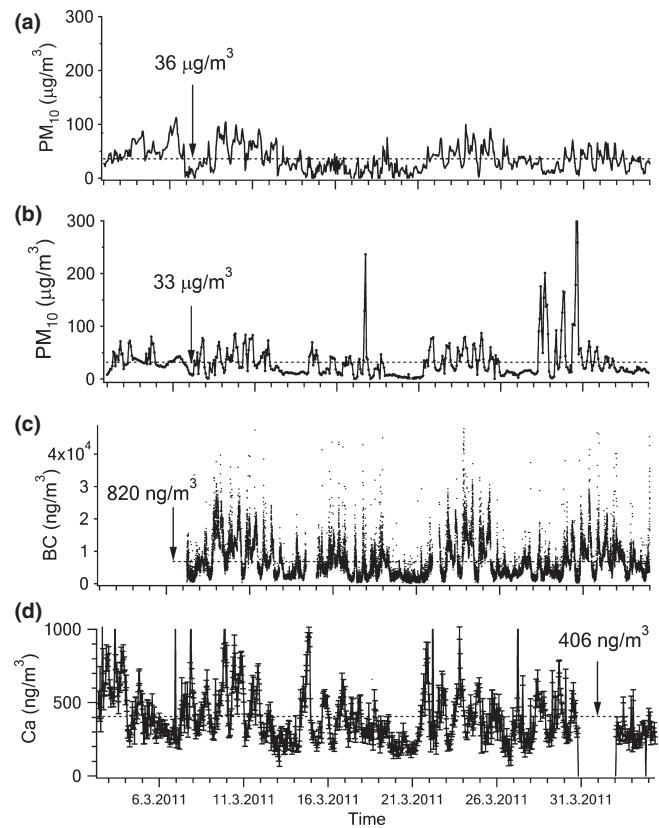


Fig. 6 (a) Outdoor PM_{10} concentration at the ARSO measuring site (half-hour average). (b) Indoor PM_{10} concentration averaged over the exercise time period (90-min average). (c) BC concentration measured just outside the gym (one-minute average). (d) Indoor Ca concentration (one-hour average). Dashed line on each graph denotes the signal average over the whole period of the monitoring

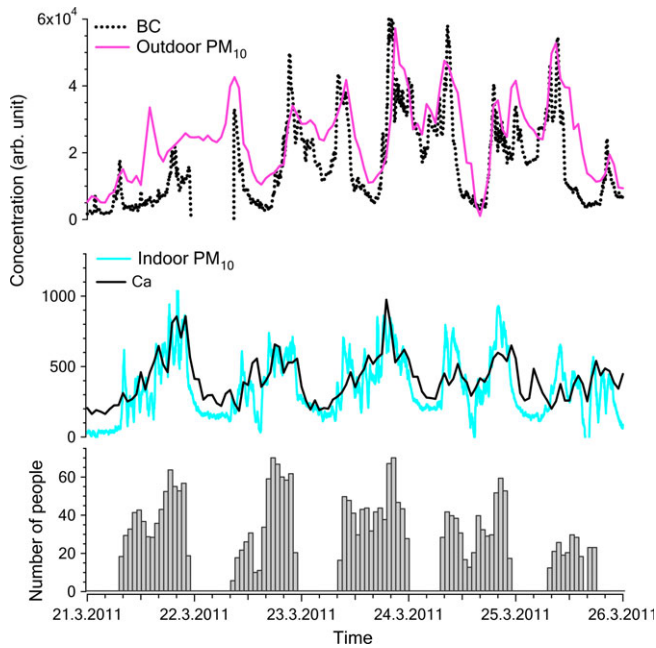


Fig. 7 Measured concentrations of outdoor PM₁₀, outdoor BC, indoor PM₁₀, and indoor Ca for the March 21 to 26, 2011 period together with the exercise attendance data

Concentration of particulate matter

Black carbon. The outdoor BC concentration trend measured just outside the gym (Figures 6c, 7) shows a rather good agreement with the ARSO half-hour average PM₁₀ signal (Figure 6a) that was acquired simultaneously (correlation factor 0.54). Small differences between the two signals can be explained by the local outdoor sources, such as car parking activities in front of the gym. Good agreement of two data sets shows that although the ARSO data were acquired at the location about 5 km away from the gym (Figure 1a), the local effects on the outdoor dust concentration were of minor importance, and the ARSO data set was taken as representative of the outdoor atmospheric conditions.

PM₁₀. We rely on statistical analysis to estimate the importance of the outdoor–indoor PM₁₀ transfer, as well as to determine type and extent of correlation between observed trends of the indoor dust concentration and human activities in the gym. As expected, auto- and cross-correlation functions of the measured signals show significant daily and weekly periodicity due to the corresponding periodicity of weather conditions and human activities such as traffic or the number of people exercising in the gym (Figure 6). On the other hand, there is a negligible correlation of the two outdoor signals (PM₁₀ and BC) with the indoor PM₁₀ signal (Figure 6b). To isolate the human exercise component, we eliminated the outdoor component from the interior PM₁₀ signal by the FastICA algorithm

based on the independent component analysis method (Širca and Horvat, 2012). FastICA decomposes measured signals (PM₁₀ outside and PM₁₀ inside) into linear combinations of uncorrelated signals and returns these along with the corresponding mixing matrix. As the variation of the indoor PM₁₀ signal already looks well correlated with the histogram of exercising people (Figure 7), it is not surprising that trends of the two uncorrelated signals came out practically equal to the trends of the two measured signals. This result shows that there was no relevant outdoor–indoor PM₁₀ transfer so that the PM₁₀ trend recorded inside the gym was mainly governed by the exercising people, in agreement with previous observations (Buonanno et al., 2012; Ramos et al., 2014). Although there was an indoor–outdoor air exchange, especially during the times of the activated HVAC, the air filtration system efficiently prevented the passage of dust, even for the local parking episodes detected by the outdoor BC signal.

To determine an average PM₁₀ particle concentration increases due to a human exercise, we have averaged the PM₁₀ signal over each of the single exercise slots and plotted the result against the number of people exercising in the gym (Figure 8). There is a substantial correlation between the two quantities (0.49), and an even larger correlation coefficient is obtained considering only the people using the B and C areas where the TEOM was placed. This points to the conclusion that at least some part of the PM₁₀ emission (the coarse fraction) had a local character, that is, the proximity of activity plays a role in the measured concentration

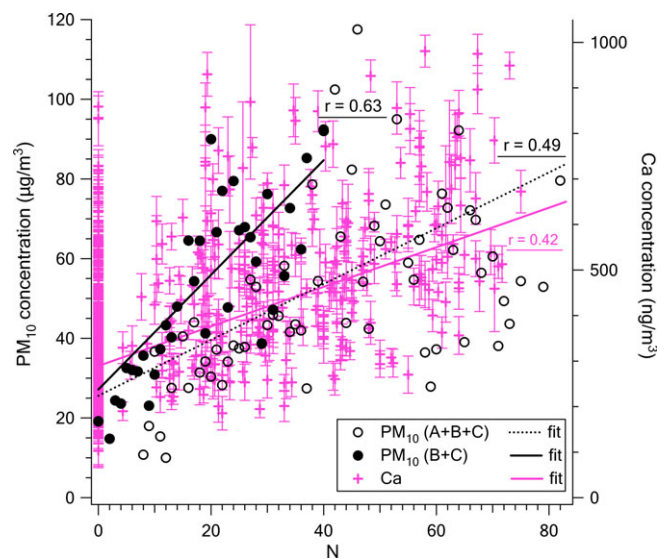


Fig. 8 PM₁₀ concentration averaged over the 90-min exercise slot versus number N of people attending exercises in areas A, B, and C (empty circles), or attending exercises in area B and C only (full circles). Crosses (pink) represent hourly Ca concentration means versus N. For each case, a linear fit (dotted black line, black line, pink line) and correlation coefficient (r) are given

values. Under these conditions, the linear fit returns an average increase of $1.5 \pm 0.3 \mu\text{g}/\text{m}^3$ of PM_{10} concentration per person per exercise slot at the measuring site (Figure 8). This means that the person attending an average exercise (~20 people using B and C areas) experienced an increase of PM_{10} concentration of about $30 \mu\text{g}/\text{m}^3$ during the exercise. Taking into account also activities on the distant area A, the measured average increase of PM_{10} concentration dropped to $0.7 \pm 0.2 \mu\text{g}/\text{m}^3$ (Figure 8) indicating partial localization of the PM_{10} signal due to the resuspension processes. On the other hand, we found that the monthly average PM_{10} concentration level in the gym ($33 \mu\text{g}/\text{m}^3$) was lower than outside ($36 \mu\text{g}/\text{m}^3$), mainly because of the lower average background PM_{10} concentration level during the weekends with no one practicing in the gym ($15 \mu\text{g}/\text{m}^3$).

Ca concentration. The measured hourly elemental concentration trend for Ca shows a clear correlation (0.42) with exercising activities in the gym (Figures 6d, 7, 8), and there is a weaker, but still significant correlation for Si. These two, the so-called earth elements, are obvious markers of exercising – despite regular daily floor cleaning by wet cloths, a layer of dust from earth was generated during exercises by abrasion of sports shoes, or previously accumulated dust on the floor was released into the air by player's movements. The net result in our case was about a two to three times higher concentration of Ca during the exercises with respect to the Ca background concentration in the gym. Similar to PM_{10} , the Ca concentration increase is observed to depend on the number of practicing people with a slope of $5 \text{ ng}/\text{m}^3$ per person. An increase of Ca concentration correlated with the people's presence was reported previously (Žitnik et al., 2010) and is typical for the indoor atmosphere. The trends of other analyzed elements such as Fe, Cr, and Cu display a few occasional spikes that may be generated by hitting the ball hard against metal constructions, such as goal frames, basketball rings, volleyball net supports, or instrument shielding, and the analysis shows no significant correlation with the number of exercising people (for Fe the correlation coefficient is 0.02).

Limitations

We did not measure CO_2 concentration in the gym although it is expected to be a strong marker of physical activity. The data acquisition of the IEQ parameters for a relatively large gym was performed at the single measuring site. Although we have detected a local character of PM resuspension, our single-point measurements, as well as an absence of knowledge about the precise HVAC operational parameters, prevented us from reliably estimating the coarse particle emission factors (Buonanno et al., 2012). The

measured data trends indicated that water vapor pressure and temperature were not constant along the gym's vertical profile (10 m), and use of multiple sensors would be more appropriate. We could not correlate observed signal levels with different types of sport activities because several of them were going on simultaneously in different areas of the gym.

Conclusions

A month-long survey of several IEQ parameters inside a gym operating a regular exercise program for students with time slots allocated for basketball, football, volleyball, badminton, boxing, and fitness was conducted. Due to these exercises, effects on the gym's IEQ were observed, such as increase of air humidity, air temperature, PM_{10} concentration, and Ca concentration. While the indoor relative humidity and dust concentration were identified as strong markers of sport activity, a rather small air temperature increase was detected because a single person's heat output was dissipated by the radiation of only a small fraction (15%), and the signal was additionally obscured by the effect of the solar irradiation heating. In this study, averages were computed: with typically 38 people attending a 90-min exercise time slot with 143 ± 10 bpm heart rate, each person evaporated 0.94 kg of water into 12500 m^3 gym volume and contributed 0.13 kWh of energy to heating the air (equivalent to 0.03 K increase of air temperature). At the same time, a single person's physical activity on the near sport areas caused a $1.5 \pm 0.3 \mu\text{g}/\text{m}^3$ rise of the PM_{10} concentration and $5 \text{ ng}/\text{m}^3$ rise of Ca concentration.

These results suggest a sportsman, on average, would experience a sixfold larger PM_{10} dose in 90 min while exercising indoors compared to the dose received while being inactive outdoors. For comparison, the study of Buonanno et al. (2012) estimated 12.9 times higher dose of the coarse PM fraction received by a 10-year-old child during one hour of physical activity in the gym compared to the dose the child would experience sitting in class. To reduce the health hazard related to the periodic extra PM exposure in the gym, it would be desirable to adjust the number of practicing people to the actual gym's IEQ parameter values which should be measured on a regular basis. The IEQ parameters can be improved by introducing efficient dust removal techniques, setting up specific rules of behavior in the gym, and optimizing HVAC systems.

Acknowledgements

This work was supported by the P1-0112 research programme of the Slovenian Research Agency. The authors thank all people helping to install the equipment and collect the data, in particular to M. Ribič, J.

Bratuž, M. Jamnik, I. Plešnar, and G. Pandurovič. We also thank to the Environmental Agency of the Republic of Slovenia for access to the atmospheric data of the

Bežigrad measuring station. This study was approved by the Republic of Slovenia National Medical Ethics Committee.

References

- Ainsworth, B.E., Haskell, W.L., Herrmann, S.D., Meckes, N., Bassett, D.R. Jr, Tudor-Locke, C., Greer, J.L., Vezina, J., Whitt-Glover, M.C. and Leon, A.S. (2011) 2011 Compendium of Physical Activities: a second update of codes and MET values, *Med. Sci. Sports Exerc.*, **43**, 1575–1581.
- Bennett, D.H., Fisk, W., Apte, M.G., Wu, X., Trout, A., Faulkner, D. and Sullivan, D. (2012) Ventilation, temperature, and HVAC characteristics in small and medium commercial buildings in California, *Indoor Air*, **22**, 309–320.
- Braniš, M., Šafrànek, J. and Hytychová, A. (2009) Exposure of children to airborne particulate matter of different size fractions during indoor physical education at school, *Build. Environ.*, **44**, 1246–1252.
- Braniš, M., Šafrànek, J. and Hytychová, A. (2011) Indoor and outdoor sources of size-resolved mass concentration of particulate matter in a school gym - implications for exposure of exercising children, *Environ. Sci. Pollut. Res.*, **18**, 598–609.
- Buonanno, G., Fuoco, F.C., Marini, S. and Stabile, L. (2012) Particle resuspension in school gyms during physical activities, *Aerosol Air Qual. Res.*, **12**, 803–813.
- Campbell, J.L., Boyd, N.I., Grassi, N., Bonnick, P. and Maxwell, J.A. (2010) The Guelph PIXE software package IV, *Nucl. Instrum. Methods B*, **268**, 3356–3363.
- Fromme, H., Twardella, D., Dietrich, S., Heitmann, D., Schierl, R., Liebl, B. and Rüden, H. (2007) Particulate matter in the indoor air of classrooms - exploratory results from Munich and surrounding area, *Atmos. Environ.*, **41**, 854–866.
- Gehin, E., Ramalho, O. and Kirchner, S. (2008) Size distribution and emission rate measurement of fine and ultrafine particle from indoor human activities, *Atmos. Environ.*, **42**, 8341–8352.
- Hansen, A.D.A., Rosen, H. and Novakov, T. (1984) The aethalometer - an instrument for real time measurement of optical absorption by aerosol particles, *Sci. Total Environ.*, **38**, 191–196.
- Klepeis, N.E., Nelson, W.C., Ott, W.R., Robinson, J.P., Tsang, A.M., Switzer, P., Behar, J.V., Hern, S.C. and Engelmann, W.H. (2001) The National Human Activity Pattern Survey (NHAPS): a resource for assessing exposure to environmental pollutants, *J. Expo. Anal. Env. Epidemiol.*, **11**, 231–252.
- Kuo, S.C., Hsieh, L.Y., Tsai, C.H. and Tsai, Y.I. (2007) Characterization of PM_{2.5} fugitivemetal in the workplaces and the surrounding environment of a secondary aluminum smelter, *Atmos. Environ.*, **41**, 6884–6900.
- Koutsoyannis, D. (2012) Clausius-Clapeyron equation and saturation vapour pressure: simple theory reconciled with practice, *Eur. J. Phys.*, **33**, 295–305.
- Martuzevičius, D., Grinshpun, S., Lee, T., Hu, S., Biswas, P., Reponen, T. and LeMasters, G. (2008) Traffic-related PM_{2.5} aerosol in residential houses: indoor versus outdoor concentrations, *Atmos. Environ.*, **42**, 6575–6585.
- Matsuyama, S., Katoh, K., Sugihara, S., Ishii, K., Yamazaki, H., Satoh, T., Ts, A., Tanaka, A., Komori, H., Hotta, K., Izukawa, D. and Mizuma, K. (2003) Multi-site aerosol monitoring using mini step sampler, *Int. J. PIXE*, **13**, 65–80.
- Mitchell, C.S., Zhang, J., Sigsgaard, T., Jantunen, M., Lioy, P.J., Samson, R. and Karol, M.H. (2007) Current state of the science: health effects and indoor environmental quality, *J. Environ. Health Persp.*, **115**, 958–964.
- Ramos, C.A., Wolterbeek, H.T. and Almeida, S.M. (2014) Exposure to indoor air pollutants during physical activity in fitness centers, *Build. Environ.*, **82**, 349–360.
- Rothman, L.S., Gordon, I.E., Barbe, A., Chris Benner, D., Bernath, P.F., Birk, M., Boudon, V., Brown, L.R., Campargue, A., Champion, J.-P., Chance, K., Coudert, L.H., Dana, V., Devi, V.M., Fally, S., Flaud, J.-M., Gamache, R.R., Goldman, A., Jacquemart, D., Kleiner, I., Lacombe, N., Lafferty, W.J., Mandin, J.-Y., Massie, S.T., Mikhailenko, S.N., Miller, C.E., Moazzen-Ahmadi, N., Naumenko, O.V., Nikitin, A.V., Orphal, J., Perevalov, V.I., Perrin, A., Predoi-Cross, A., Rinsland, C.P., Rotger, M., Šimečková, M., Smith, M.A.H., Sung, K. and Tashkun, S.A. (2009) The HITRAN 2008 molecular spectroscopic database, *J. Quant. Spectrosc. Radiat.*, **110**, 533–572.
- Routledge, H. C. and Ayers, J.G. (2006) Cardiovascular effects of particles, *Air Pollut. Rev.*, **3**, 19–42.
- Sacks, D.E. and Shendell, D.G. (2014a) Case Study: Particle Concentrations at a Local Gym Dependent on Mechanical Ventilation in a Retrofitted Industrial Building in Central NJ. Proceedings, Indoor Air 2014, July 7–12, Hong Kong, China.
- Sacks, D.E. and Shendell, D.G. (2014b) Case Study: Ventilation and Thermal Comfort Parameter Assessment of a Local Gym Dependent on Mechanical Ventilation in a Retrofitted Industrial Building in Central NJ. Proceedings, Indoor Air 2014, July 7–12, Hong Kong, China.
- Salma, I., Dosztály, K., Borsòs, T., Söveges, B., Weidinger, T., Kristóf, G., Pèter, N. and Sz, K. (2013) Physical properties, chemical composition, sources, spatial distribution and sinks of indoor aerosol particles in a university lecture hall, *Atmos. Environ.*, **64**, 219–228.
- Schweizer, C., Edwards, R.C., Bayer-Oglesby, L., Gauderman, W.J., Ilacqua, V., Jantunen, M.J., Laie, H.K., Nieuwenhuijzen, M. and Künzli, M. (2007) Indoor time-microenvironment-activity patterns in seven regions of Europe, *J. Expo. Anal. Env. Epidemiol.*, **17**, 170–181.
- See, S.W. and Balasubramanian, R. (2008) Chemical characteristics of fine particles emitted from different gas cooking methods, *Atmos. Environ.*, **42**, 8852–8862.
- Seppänen, O.A., Fisk, W.J. and Mendell, M.J. (1999) Association of ventilation rates and CO₂ concentrations with health and other responses in commercial and institutional buildings, *Indoor Air*, **9**, 1921–1930.
- Shapiro, Y., Pandolf, K.B. and Goldman, R.F. (1982) Predicting sweat loss response to exercise, environment and clothing, *Eur. J. Appl. Physiol.*, **48**, 83–96.
- Širca, S. and Horvat, M. (2012) *Computational Methods for Physicists*, Berlin Heidelberg, Springer-Verlag.
- Sotiriou, M., Ferguson, S.F., Davey, M., Wolfson, J.M., Demokritou, P., Lawrence, J., Sax, S.N. and Koutrakis, P. (2008) Measurement of particle concentrations in a dental office, *Environ. Monit. Assess.*, **137**, 351–361.
- Žitnik, M., Kastelic, A., Rupnik, Z., Pelicon, P., Vaupetič, P., Bučar, K., Novak, S., Samardžija, Z., Matsuyama, S., Catella, G. and Ishii, K. (2010) Time-resolved measurements of aerosol elemental concentrations in indoor working environments, *Atmos. Environ.*, **44**, 4954–4963.